

Supplemental Material

Anti-bubbles and fine cylindrical sheets of air

by Beilharz, Guyon, Li, Thoraval & Thoroddsen

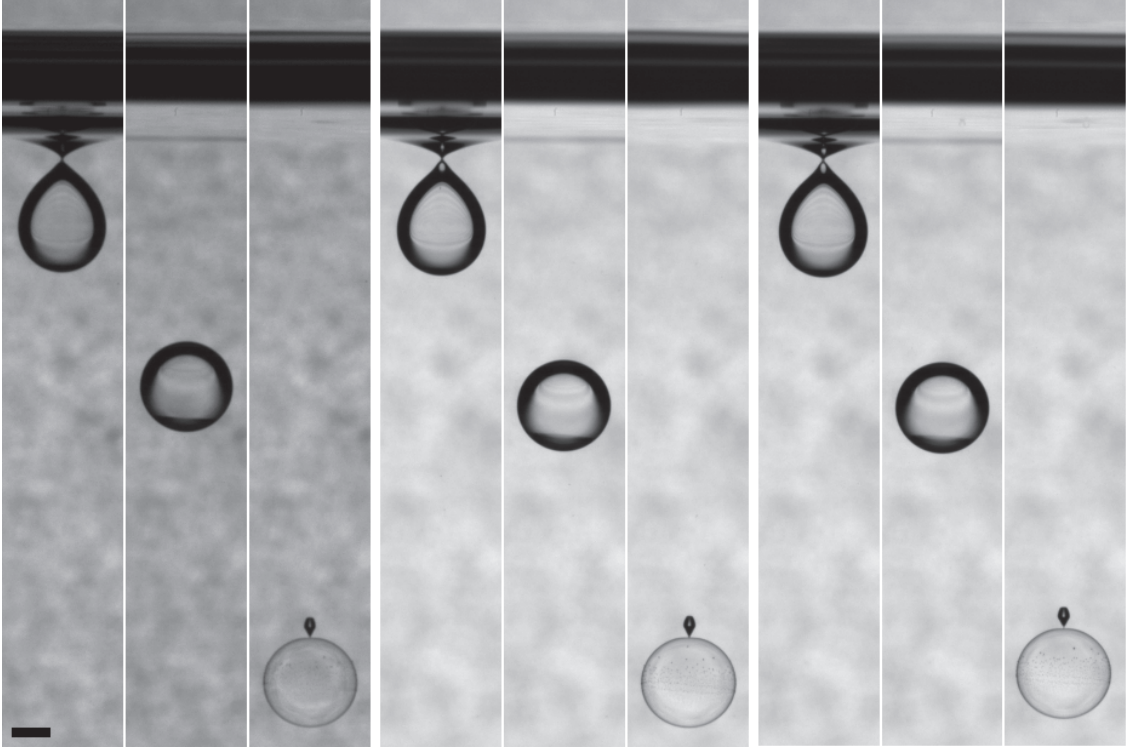


FIGURE 22. Typical repeatability of the anti-bubble formation, for $\nu_d = 500$ cSt drop and the pool is $\nu_p = 1$ cSt. The impact height is $H = 15$ mm. From left to right, the first frames show the pinch-off which forms the anti-bubble, occurring at $t = 31.15, 31.04$ & 31.47 ms after the drop reaches the pool surface. The center frames are all at $t = 150$ ms and the last frames show the end of the breakup of the air-shell, occurring at $245.9, 242.2$ & 254.4 ms. The scale bar is 1 mm.

1. Repeatability

Figure 22 compares three consecutive realizations under exactly the same impact conditions, to quantify the repeatability of the formation and breakup of anti-bubbles. The surface shapes are identical during the pinch-off of the air cavity around the drop thus forming the antibubble and the breakup of the spherical air-shell starts at the bottom propagating around the drop, finally pinching off a small bubble on the top of the drop. The timings are also quite repeatable, with the maximum difference in the overall timing of less than 5%.

Figure 23 highlights two features in the interference patterns of light passing through the anti-bubble and the drop, taken from the sequences in Fig. 22. Keep in mind that the index of refraction differs between the drop and pool liquids. Right at the pinch-off there is a clear lower boundary where interference patterns begin, as indicated by the arrow in the first frame. This boundary moves steadily up the drop. The second boundary emerges from the bottom as a darker region, which also moves steadily up the drop. The rupture of the film starts at the bottom and propagates upwards. The resulting bubble distribution indicates that these two boundaries mark transitions in the film thickness, with the thinnest region at the bottom, with the finest micro-bubbles. When the rupture travels past the lower boundary it leaves a well-defined ring of bubbles, marked by the arrow in the last frame. Above this ring, larger bubbles are observed, until the edge

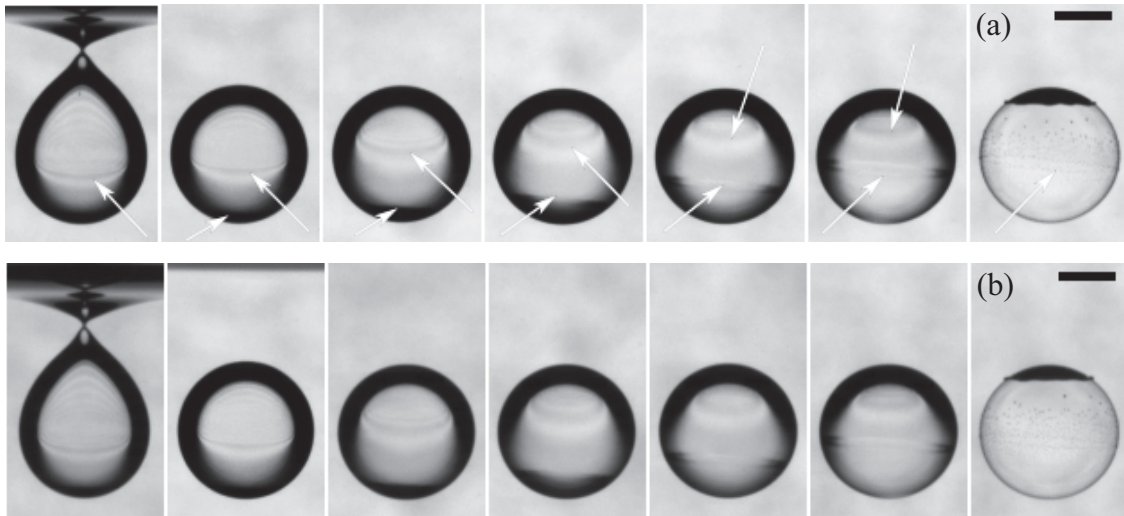


FIGURE 23. Close-up images following the drop, for two adjacent realizations. Interference patterns observed in the light transmitted through the anti-bubble, shows how the bottom section of the bubble-shell thins. The arrows highlight two prominent features in the light patterns. The scale bar is 1 mm.

reaches the upper boundary, where the air layer stops shedding bubbles and contracts into a bubble at the top (last frames in Fig. 22).

Besides these qualitative information, it is possible to extract quantitative information about the layer thickness from these interference patterns, using interferometry, as shown in section 3.7.

Figure 24 shows an impact condition where the drop rebounds. The surface goes through large deformation, but net curvature of the neck is either positive or the inner liquid prevents pinch-off, thus allowing surface tension to pull the drop back up. The rebounding shows differences between the two sequences (compare shapes for $t = 53.6$ ms), perhaps due to the viscous stress in the thread, during compression and buckling.

Buoyancy plays no role in the rebounding, as the density of the drop is larger than the pool and the volume of the air-sheath is minimal.

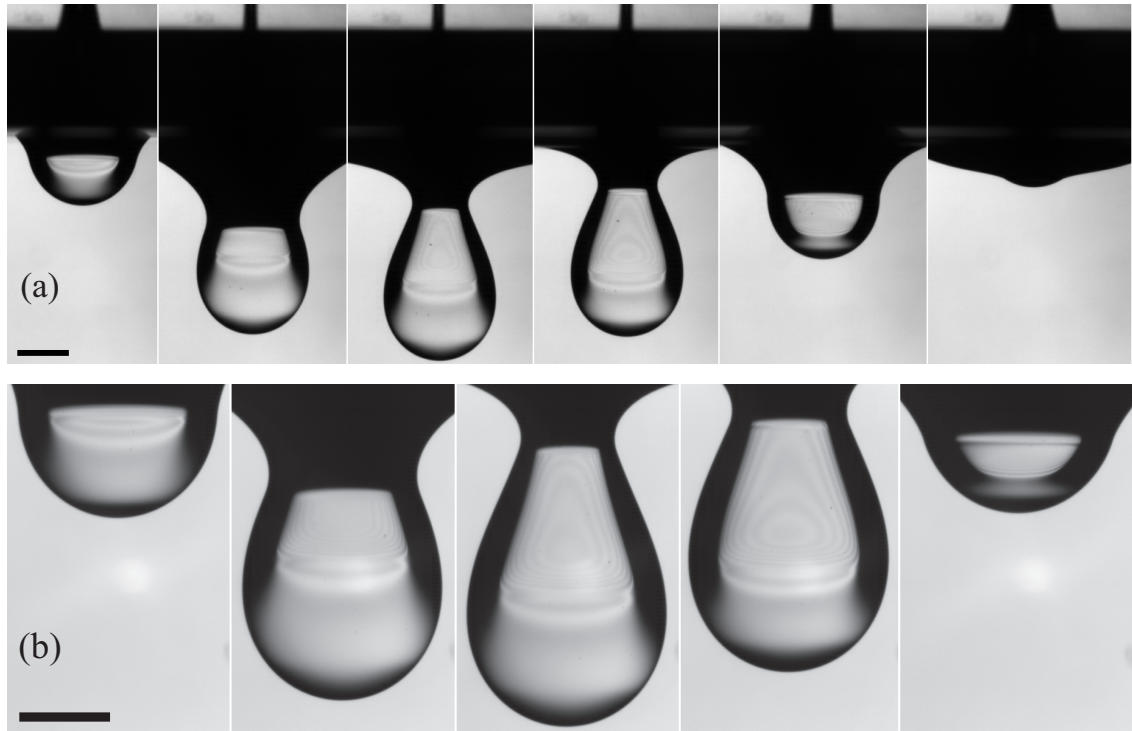


FIGURE 24. Repeatability during large surface deformations and rebound of a drop, for $\nu_d = 10,000$ cSt and $\nu_p = 10$ cSt, from $H = 27.5$ mm. Times shown at (a) $t = 3.3, 14.3, 25.3, 39.5, 53.6$ & 61.1 ms, (b) $t = 3.3, 14.3, 25.3, 39.5$ & 53.6 ms after the drop reaches the pool surface. The scale bars are 1 mm.

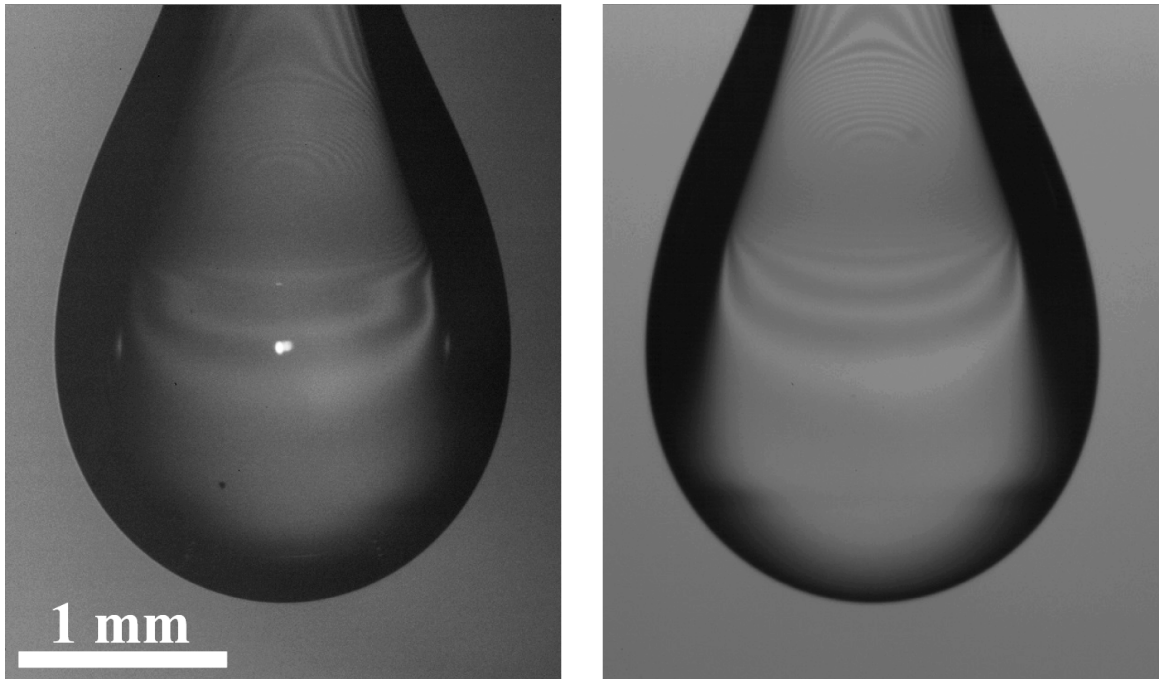


FIGURE 25. Comparison of interference patterns observed with a (a) front and (b) back monochromatic lighting setup, as shown in Fig. 2 (b,c). For $\nu_d = 10,000$ cSt and $\nu_p = 1$ cSt, from $H = 25.5$ mm.

2. Interferometry

Figure 25 compares the fringes, for identical impact conditions, but observed using front and back monochromatic lighting-setup, as sketched in Fig. 2(b,c). The front-lighting is darker and has a bright reflection spot, but the fringe patterns shows no significant differences.